Ultra-high quality factor planar Si_3N_4 ring resonators on Si substrates

Ming-Chun Tien,* Jared F. Bauters, Martijn J. R. Heck, Daryl T. Spencer, Daniel J. Blumenthal, and John E. Bowers

Department of Electrical and Computer Engineering, University of California, Santa Barbara, CA 93106, USA
**jtien@ece.ucsb.edu*

Abstract: We demonstrate planar Si_3N_4 ring resonators with ultra-high quality factors (Q) of 19 million, 28 million, and 7 million at 1060 nm, 1310 nm, and 1550 nm, respectively. By integrating the ultra-low-loss Si_3N_4 ring resonators with laterally offset planar waveguide directional couplers, optical add-drop and notch filters are demonstrated to have ultra-narrow bandwidths of 16 MHz, 38 MHz, and 300 MHz at 1060 nm, 1310 nm, and 1550 nm, respectively. These are the highest Qs reported for ring resonators with planar directional couplers, and ultra-narrowband microwave photonic filters can be realized based on these high-Q ring resonators.

OCIS codes: (130.0130) Integrated optics; (230.5750) Resonators; (230.7390) Waveguides, planar; (230.7408) Wavelength filtering devices.

References and links

1. V. Lefevre-Seguin and S. Haroche, "Towards cavity-QED experiments with silica microspheres," Mater. Sci. Eng., B **B48**, 53–58 (1997).
2. D. W. Vernooy, A. Furusawa, N. P. Georgiades, V. S. Ilchenko, and H. J. Kimble, "Cavity QED with high-Q whispering gallery modes," Phys. Rev. A **57**, R2293–R2296 (1998).
3. S. M. Spillane, T. J. Kippenberg, and K. J. Vahala, "Ultralow-threshold Raman laser using a spherical dielectric microcavity," Nature **415**(6872), 621–623 (2002).
4. F. Vollmer, D. Braun, A. Libchaber, M. Khoshsima, I. Teraoka, and S. Arnold, "Protein detection by optical shift of a resonant microcavity," Appl. Phys. Lett. **80**(21), 4057–4059 (2002).
5. L. Maleki, A. B. Matsko, A. A. Savchenkov, and V. S. Ilchenko, "Tunable delay line with interacting whispering-gallery-mode resonators," Opt. Lett. **29**(6), 626–628 (2004).
6. D. Geuzebroek, E. Klein, H. Kelderman, N. Baker, and A. Driessen, "Compact wavelength-selective switch for gigabit filtering in access networks," IEEE Photon. Technol. Lett. **17**(2), 336–338 (2005).
7. E. J. Klein, D. H. Geuzebroek, H. Kelderman, S. Gabriel, N. Baker, and A. Driessen, "Reconfigurable optical add-drop multiplexer using microring resonators," IEEE Photon. Technol. Lett. **17**(11), 2358–2360 (2005).
8. M. S. Rasras, T. Kun-Yii, D. M. Gill, C. Young-Kai, A. E. White, S. S. Patel, A. Pomerene, D. Carothers, J. Beattie, M. Beals, J. Michel, and L. C. Kimerling, "Demonstration of a tunable microwave-photonic notch filter using low-loss silicon ring resonators," J. Lightwave Technol. **27**(12), 2105–2110 (2009).
9. P. Dong, N. N. Feng, D. Feng, W. Qian, H. Liang, D. C. Lee, B. J. Luff, M. Asghari, A. Agarwal, T. Banwell, R. Menendez, P. Toliver, and T. K. Woodward, "A tunable optical channelizing filter using silicon coupled ring resonators," in *2010 Conference on Lasers and Electro-Optics (CLEO)* (IEEE, San Jose, CA, USA, 2010).
10. D. K. Armani, T. J. Kippenberg, S. M. Spillane, and K. J. Vahala, "Ultra-high-Q toroid microcavity on a chip," Nature **421**(6926), 925–928 (2003).
11. M. Soltani, S. Yegnanarayanan, and A. Adibi, "Ultra-high Q planar silicon microdisk resonators for chip-scale silicon photonics," Opt. Express **15**(8), 4694–4704 (2007).
12. I. Goykhman, B. Desiatov, and U. Levy, "Ultrathin silicon nitride microring resonator for biophotonic applications at 970 nm wavelength," Appl. Phys. Lett. **97**(8), 081108 (2010).
13. A. Gondarenko, J. S. Levy, and M. Lipson, "High confinement micron-scale silicon nitride high Q ring resonator," Opt. Express **17**(14), 11366–11370 (2009).
14. E. Shah Hosseini, S. Yegnanarayanan, A. H. Atabaki, M. Soltani, and A. Adibi, "High quality planar silicon nitride microdisk resonators for integrated photonics in the visible wavelength range," Opt. Express **17**(17), 14543–14551 (2009).
15. J. F. Bauters, M. J. R. Heck, D. John, D. Dai, M.-C. Tien, J. S. Barton, A. Leinse, R. G. Heideman, D. J. Blumenthal, and J. E. Bowers, "Ultra-low-loss high-aspect-ratio Si_3N_4 waveguides," Opt. Express **19**(4), 3163–3174 (2011).

#146129 - $15.00 USD Received 18 Apr 2011; revised 22 May 2011; accepted 27 May 2011; published 29 Jun 2011

16. J. F. Bauters, M. J. R. Heck, D. John, M.-C. Tien, A. Leinse, R. G. Heideman, D. J. Blumenthal, and J. E. Bowers, "Ultra-low loss silica-based waveguides with millimeter bend radius," in *Proceedings of ECOC* (Torino, Italy, 2010).
17. D. Dai, Z. Wang, J. F. Bauters, M.-C. Tien, M. J. R. Heck, D. J. Blumenthal, and J. E. Bowers, "Polarization characteristics of low-loss nano-core buried optical waveguides and directional couplers," in *Group IV Photonics (GFP), 2010 7th IEEE International Conference on* (2010), pp. 260–262.
18. D. Dai, Z. Wang, J. F. Bauters, M.-C. Tien, M. J. R. Heck, D. J. Blumenthal, and J. E. Bowers, "Low-loss Si_3N_4 arrayed-waveguide grating (de)multiplexer using nano-core optical waveguides," (to be published).
19. J. E. Heebner, T. C. Bond, and J. S. Kallman, "Generalized formulation for performance degradations due to bending and edge scattering loss in microdisk resonators," Opt. Express **15**(8), 4452–4473 (2007).

1. Introduction

Ultra-high-Q optical resonators are crucial to an assortment of applications including cavity quantum electrodynamics [1,2], nonlinear optics [3], bio-sensing [4], telecommunications [5–7], and microwave photonic filters [8,9]. Most ultra-high-Q resonators use tapered fiber coupling to a dielectric toroid or sphere. The wafer-scale production of our planar coupled resonators through standard processing techniques offers greater fabrication control while also opening up the possibility of integration. Indeed, an ideal platform for these resonators-on-a-chip would combine ultra-high-Q with planar processing capability, lasers, photodetectors and other photonic components for integration, and transparency across a wide range of wavelengths. Integration allows for increased functionality along with lower cost, while transparency permits resonator operation in the wavelength regime most suitable to the application.

Of the various materials available for fabricating a resonator-on-a-chip, SiO_2, silicon-on-insulator (SOI), and Si_3N_4 are good candidates because of their use in low-loss planar optical waveguides. Whispering-gallery-mode (WGM) resonators with ultra-high quality factor (Q) of 100 million have been demonstrated in microtoroidal structures made from thermally grown silica [10]. However, due to their nonplanar structure, it is difficult to integrate such resonators with other optical devices for complex functionality. Planar silicon microdisk resonators integrated with in-plane waveguides were reported to have Qs of 3 million at 1550 nm [11]; however, the resonance is in a high-order mode, and silicon is not transparent in the 750~1000 nm wavelength regime, which is important for some applications such as bio-sensing due to the low optical absorption in water and the transparency of proteins in this wavelength range [12]. In the Si_3N_4 on SiO_2 platform, microring resonators with integrated directional couplers were demonstrated to have Qs up to 3 million at 1550 nm [13], while microdisk resonators have Qs of 3.4 million at 652-660 nm [14]. Though transparent and planar, the quality factor of such Si_3N_4 on SiO_2 resonators must be increased to meet the performance demands of many applications.

In this paper, we demonstrate planar Si_3N_4 ring resonators with record-high Qs in the 1060, 1310, and 1550 nm wavelength regimes. The resonators are fabricated with recently demonstrated ultra-low-loss high-aspect-ratio waveguide technology [15] and have integrated directional couplers. Additional photonic components for integration, including multi-mode interferometers, Mach-Zehnder interferometers, polarizers, and arrayed-waveguide gratings [15–18], have been demonstrated on this platform. We begin with a review of the ring resonator design (Section 2). We then describe the characterization method used to obtain the transmission spectrum of the resonators with adequate resolution (Section 3). Finally, we discuss the suitability of these ultra-high-Q resonators with planar directional couplers for a specific application, namely ultra-narrowband filters (Section 4).

2. Design of high-Q ring resonators

The design of high-aspect-ratio Si_3N_4-core and SiO_2-cladding waveguides is discussed in [15]. A general rule to reduce the scattering loss is to expand the effective optical mode by reducing the core thickness and thus decrease the overlap between the mode and the core-cladding interface. We have demonstrated 2.9 dB/m of propagation loss for 2.8-μm-wide and 80-nm-

#146129 - $15.00 USD Received 18 Apr 2011; revised 22 May 2011; accepted 27 May 2011; published 29 Jun 2011

thick Si_3N_4 waveguides at 1550 nm. Using this type of waveguide to construct ring resonators, ultra-high-Q can be achieved.

Figure 1 shows the theoretical Si_3N_4 waveguide loss including the scattering and bending loss contributions for different bend radii at different wavelengths. The rms sidewall and surface roughness used for the calculations are 4.75 nm and 0.175 nm, while the correlation lengths are 50 nm and 30 nm, respectively. The surface and sidewall roughness parameters are measured using an atomic force microscope (AFM) and a scanning electron microscope (SEM), respectively. In order to realize high-Q ring resonators, the bend radii of the ring resonators have to be large enough to avoid the dominant bending loss. The model shows that the optical mode is better confined at shorter wavelengths and thus allows smaller bend radius without bending loss; however, the scattering loss at shorter wavelengths is higher [19]. For 5.3-μm-wide and 50-nm-thick Si_3N_4 waveguides, the radii have to be larger than 7 mm, 3 mm, and 2 mm in 1550nm, 1310nm, and 1060nm wavelength regimes to have negligible bending loss, and their corresponding scattering-limited losses are 0.4 dB/m, 0.8 dB/m, and 2.1 dB/m. In order to reduce the size of the ring resonators at 1550 nm, 2.8-μm-wide and 80-nm-thick waveguides (the black line in Fig. 1) are used to provide better optical confinement, resulting in negligible bending loss for radii larger than 1.5 mm. The experimental data points, which will be described in the next section, are also indicated as circles for 5.3-μm-wide and 50-nm-thick Si_3N_4 waveguides and as crosses for 2.8-μm-wide and 80-nm-thick waveguides.

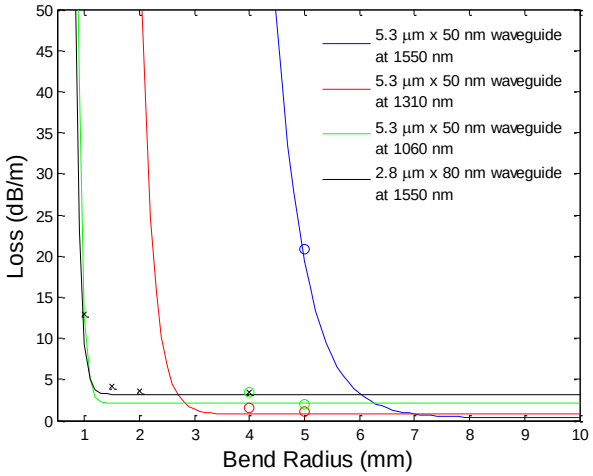

Fig. 1. Waveguide loss for different waveguide geometries in different wavelength regimes. Solid lines represent theoretical loss values while the circles and crosses indicate the experimental data. The rms deviation of sidewall and surface roughness used for calculation are 4.75 nm and 0.175 nm, while the correlation lengths are 50 nm and 30 nm, respectively [15].

3. Optical characterization of high-Q ring resonators

3.1 Measurement setup

The high-Q ring resonators are characterized by measuring the transmission spectra in three different wavelength regimes to understand the sources of loss. In order to resolve the transmission spectrum of such high-Q ring resonators, a low-linewidth laser source capable of continuous wavelength scanning and a synchronized oscilloscope are used, as shown in Fig. 2. A tunable laser is used as a laser source, followed by a polarization controller and a lensed fiber to couple the light into the waveguide. The input polarization is set at the transverse electric (TE) mode because the ring resonator is designed to have high polarization extinction ratio, and the transverse magnetic (TM) mode has much higher loss than the TE mode [17]. Another lensed fiber is used to collect the transmission power from the waveguide output and

#146129 - $15.00 USD Received 18 Apr 2011; revised 22 May 2011; accepted 27 May 2011; published 29 Jun 2011

send it to a photodetector attached to the oscilloscope. The photodetector then converts the transmission spectrum from the wavelength to the time domain, and the spectrum is displayed on the oscilloscope. By adjusting the wavelength scanning speed and oscilloscope sampling rate, a high-resolution spectrum can be achieved, and it is only limited by the laser linewidth. The tunable laser used in the 1550 nm regime is an Agilent 81600B laser module, which has a laser linewidth of 100 kHz. In the 1060 and 1310 nm regimes, we use Thorlabs external cavity tunable lasers. Because of the long external cavity, the lasers have linewidths less than 130 kHz.

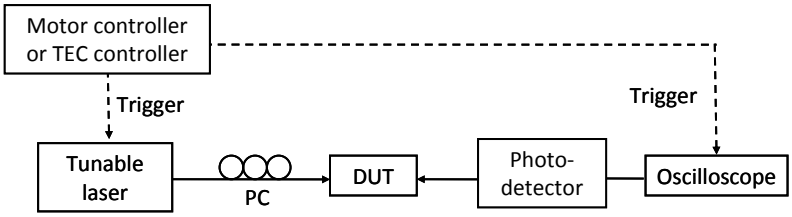

Fig. 2. A measurement setup for high-Q ring resonators. Different tunable lasers are used for measurement in the 1060 nm, 1310 nm, and 1550 nm wavelength regimes. PC: polarization controller; DUT: device under test.

3.2 Characterization of ring resonators at 1060 nm, 1310 nm, and 1550 nm

In order to find out the optimal waveguide geometry for different wavelengths, ring resonators with different bend radii (1 mm, 1.5 mm, 2 mm, 4 mm, and 5 mm) and Si_3N_4 core thicknesses (40 nm, 50 nm, and 80 nm) were fabricated. The ring resonators have 15-μm-thick SiO_2 cladding for 40- and 50-nm-thick Si_3N_4 cores, and 8-μm-thick cladding for 80-nm-thick cores to prevent optical leakage to the silicon substrate. Bending loss of the ring resonators is reduced with larger radius while the scattering loss is reduced with thinner waveguide cores. With measured transmission spectra of the ring resonators, waveguide losses and Qs of different ring resonators can be extracted by curve fitting. The intrinsic Q is obtained by comparing the spectra of similar resonator structures with various power coupling ratios as in [15].

Table 1 summarizes the waveguide losses and the intrinsic Qs of the different ring resonator designs. The waveguide width for the 40 and 50-nm-thick waveguide designs is 5.3 μm. At 1060 nm, the optimal waveguide thickness for 5-mm-radius ring resonators is between 40 and 50 nm where the bending loss and scattering loss are comparable. 4-mm-radius ring resonators have higher bend radiation and bend-mode scattering loss contributions due to the tighter bend. At 1310 nm, the optical mode confinement is rather poor in the 40-nm-thick ring resonators and thus the loss is much larger than our designed power coupling from a straight waveguide to the ring resonator. As a result, no resonance dip is observed in the transmission spectra. For 50-nm-thick ring resonators, 5-mm-radius rings show higher Q than the 4-mm-radius rings due to smaller bend-associated losses. At 1550 nm, no transmitted power is observed in the 40-nm-thick waveguide due to large optical leakage to the substrate. For the 50-nm-thick ring resonators, the loss is larger than that at shorter wavelengths because of larger bending loss contribution due to lower optical confinement. Figure 1 indicates that the radius should be larger than 7 mm to eliminate the bending loss. In order to make more compact high-Q ring resonators at 1550 nm, waveguides are fabricated to be 2.8 μm wide and 80 nm thick. The increased mode confinement of these structures allows bend radii as small as 1.5 mm with negligible bending loss, as shown in Fig. 1.

#146129 - $15.00 USD Received 18 Apr 2011; revised 22 May 2011; accepted 27 May 2011; published 29 Jun 2011

Table 1. Summary of Intrinsic Qs and Waveguide Losses of Different Rings

	1550 nm	1310 nm	1060 nm
R=5mm, t=40nm, w=5.3μm	No transmitted power *	High loss **	Q=18 million
			2.1 dB/m
R=5mm, t=50nm, w=5.3μm	Q=1 million	Q=28 million	Q=19 million
	20.8 dB/m	1.1 dB/m	2.0 dB/m
R=4mm,t=50nm, w=5.3μm	High loss **	Q=21 million	Q=11 million
		1.5 dB/m	3.5 dB/m
R=2mm,t=80nm, w=2.8μm	Q=7 million	Multi-mode ***	Multi-mode ***
	2.9 dB/m		

*No transmitted power was observed through a straight waveguide due to large optical leakage to the substrate.

**The loss is too large to be extracted by ring resonance spectra. No resonance spectra are observed.

***The waveguide dimensions cause the waveguide to be strongly multi-mode at the given wavelength.

4. Ultra-high Q ring resonators as ultra-narrowband filters

These ultra-high Q ring resonators are integrated with laterally offset planar directional couplers to construct optical notch and add-drop filters with ultra-narrow bandwidths for microwave photonic filter and high-sensitivity sensor applications. As described in the previous section, the highest-Q ring resonators measured in the 1060 nm wavelength regime are 5 mm in radius and 40-50 nm in thickness. These ring resonators have Qs of 18-19 million, the highest reported for planar ring resonators at 1060 nm. Figure 3(a) shows the transmission spectrum of an optical notch filter made by a coupled waveguide and ring resonator with a thickness of 40 nm. With a power coupling of 0.8% from the waveguide to the resonator, the filter shows an ultra-narrow bandwidth of 16 MHz. In order to be used as a biosensor, a large fraction of the 15 μm upper cladding would have to be replaced with a low-refractive-index fluid. If such a structural modification does not greatly diminish the performance of these resonators, the high-Q can dramatically enhance the sensitivity of ring resonator-based sensors.

In the 1310 nm wavelength regime, the dimension of the ring resonator is chosen to be 5 mm in radius and 50 nm in thickness according to Table 1. The transmission spectrum of an optical notch filter made by this ring resonator is shown in Fig. 3(b). By curve-fitting the spectrum, the intrinsic Q of the resonator is ~28 million with corresponding propagation loss of 1.1 dB/m. The resonator is operated in the under-coupled regime with the power coupling ratio of 0.55%. As a result, the bandwidth of the filter is as narrow as 38 MHz.

In the 1550 nm wavelength regime, the ring resonators are made up of 2.8-μm-wide and 80-nm-thick waveguides, which have propagation loss as low as 2.9 dB/m [15]. The thicker waveguide core allows tighter bending to reduce the footprint of devices. Utilizing such low-loss waveguides to make a 2-mm-radius ring resonator, we achieved an intrinsic Q of 7 million. An optical add-drop filter is constructed with two waveguides coupled to the ring resonator. Figure 3(c) shows the measured transmission spectra at the through and drop ports. The resonator is operated in the over-coupled regime to reduce the insertion loss (1.2 dB in this design) at the drop port. By fitting the transmission spectra, the power coupling ratio from the waveguide to the ring resonator is estimated to be ~5% while the round-trip loss in the ring is ~1%. The resulting 3dB bandwidth of the filter is approximately 300 MHz. This passband can be used as a microwave photonic filter for channel selection.

#146129 - $15.00 USD Received 18 Apr 2011; revised 22 May 2011; accepted 27 May 2011; published 29 Jun 2011

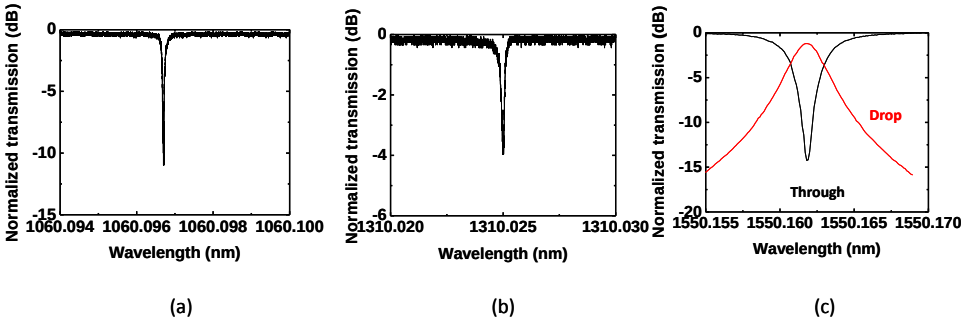

Fig. 3. (a) Transmission spectrum of an optical notch filter at 1060 nm. The radius of the ring is 5 mm with waveguide width of 5.3 μm and thickness of 40 nm (b) Transmission spectrum of an optical notch filter at 1310 nm. The radius of the ring is 5 mm with waveguide width of 5.3 μm and thickness of 50 nm (c) Transmission spectrum of an optical add-drop filter at 1550 nm. The radius of the ring is 1.5 mm with waveguide width of 2.8 μm and thickness of 80 nm.

5. Conclusions

We have demonstrated ultra-high Q ring resonators with planar directional couplers in different wavelength regimes. The intrinsic Qs of the ring resonators are 19 million, 28 million and 7 million at 1060 nm, 1310 nm, and 1550 nm, respectively. To the best of our knowledge, these are the highest Qs reported for planar ring resonators with laterally offset coupled input and output waveguides. With different integrated waveguide configurations, the rings can construct optical add-drop, optical bandpass, and optical notch filters. We demonstrated optical add-drop filters in the 1550 nm regime with a narrow bandwidth of 300 MHz and optical notch filters in the 1310 and 1060 nm regimes with ultra-narrow bandwidths of 38 MHz and 16 MHz. These ultra-high-Q planar ring resonators can be integrated with other photonic devices for complex functionality in ultra-narrowband microwave photonic filters, optical signal processing, and highly sensitive biosensor applications.

Acknowledgments

The authors thank Scott Rodgers, Jock Bovington, and Demis John for helpful discussions and LioniX BV for fabrication. This work is supported by DARPA MTO under iPhoD contract No: HR0011-09-C-0123.

#146129 - $15.00 USD Received 18 Apr 2011; revised 22 May 2011; accepted 27 May 2011; published 29 Jun 2011